

A Photoactivated Artificial Muscle Model Unit: Reversible, Photoinduced Sliding of Nanosheets

Yu Nabetani,[†] Hazuki Takamura,[†] Yuika Hayasaka,[†] Tetsuya Shimada,[†] Shinsuke Takagi,[†] Hiroshi Tachibana,[†] Dai Masui,[†] Zhiwei Tong,[‡] and Haruo Inoue^{*,†}

[†]Department of Applied Chemistry, Graduate School of Urban Environmental Sciences, Tokyo Metropolitan University, 1-1 Minami-ohsawa, Hachioji, Tokyo 192-0397, Japan, and SORST, Japan Science and Technology (JST)

[‡]Department of Chemical Engineering, Huaihai Institute of Technology, Lianyungang 222005, People's Republic of China

 Supporting Information

ABSTRACT: A novel photoactivated artificial muscle model unit is reported. Here we show that organic/inorganic hybrid nanosheets reversibly slide horizontally on a giant scale and the interlayer spaces in the layered hybrid structure shrink and expand vertically by photoirradiation. The sliding movement of the system on a giant scale is the first example of an artificial muscle model unit having much similarity with that in natural muscle fibrils. In particular, our layered hybrid molecular system exhibits a macroscopic morphological change on a giant scale (~1500 nm) relative to the molecular size of ~1 nm by means of a reversible sliding mechanism.

Photoresponsive materials have been attracting much attention in various fields such as chemistry, electronics, information technology, and medical science. Such materials, whose macroscopic-scale morphologies are reversibly changed by photoirradiation, are promising as potential materials for the application of light-driven actuators and artificial muscles. Morphological changes of organic single crystals and liquid polymer films have been reported to be reversibly induced by photoirradiation.^{1–5} Photochromic compounds such as diarylethene and azobenzene derivatives, which show a large change in the dielectric property upon photochemical reaction, have been widely studied because of their potential application for optical data storage materials.^{1–7} On the other hand, the structural or conformational changes undergone by the molecules that are induced by photochemical reactions influence the morphology of materials containing these photochromic compounds. Such photoresponsive materials have shown promise as materials for surface relief grating^{8–11} and light-driven actuators.^{1,3–5,12–14} Recently, there have appeared many reports about morphological changes of photoresponsive materials induced by photoirradiation. For example, Irie and co-workers¹ demonstrated rapid, reversible shape changes of molecular single crystals upon photoirradiation. Single crystals of diarylethene derivatives change their form from square to lozenge-shaped upon irradiation with UV and visible light. Furthermore, Ikeda and co-workers^{3–5} have found that a macroscopic morphological change of a liquid-crystal polymer film can be successfully induced by a combination of the photoisomerization reaction of azobenzene with the liquid-crystal properties. In these cases, the accumulation of many miniscule conformational changes on the molecular

scale gives rise to large morphological changes, which are much different from those in animal muscle. On the other hand, we found that upon photoirradiation of a layered hexaniobate intercalated with a polyfluoroalkyl azobenzene derivative, a very large magnitude lateral movement (sliding) of the nanosheets was reversibly induced, as clearly observed on a cross-cut section of the layered hybrid film, as a result of the concomitant reversible trans–cis isomerization of the azobenzene moiety. The total reversible sliding motion of the layered hybrid film reached ~1500 nm in the lateral direction. Furthermore, the thickness of the hybrid film (~450 nm) was reversibly changed up to ±18 nm as each interlayer space shrank and expanded because of the photoisomerization of the intercalated azobenzene derivative. The sliding movement of the system on a giant scale is the first example of an artificial muscle model having much similarity with that in natural muscle fibrils.

Layered potassium hexaniobate was synthesized by heating a 2.1:3.0 molar mixture of Nb₂O₅ (Kanto Chemical) and K₂CO₃ (Kanto Chemical) at 1373 K for 10 h, following a previous procedure described by Nassau et al.¹⁵ The polyfluoroalkyl azobenzene cationic surfactant *trans*-[2-(2,2,3,3,4,4,4-heptafluorobutylamino)ethyl]{2-[4-(4-hexylphenylazo)phenoxy]ethyl} dimethylammonium bromide (abbreviated as C3F-Azo), whose chemical structure is shown in Figure 1b, was originally synthesized [see Supporting Information (SI)-1] The hybrid nanosheet-stacked films were fabricated by intercalation exclusively into the interlayer I of the layered hexaniobate with a two-step guest–guest ion-exchange method using (MV²⁺)_xK_{4-x}Nb₆O₁₇ (MV²⁺ = methyl viologen) as a precursor (Figure 1a,b). A suspension of hexaniobate nanosheets, which were exfoliated by mixing MV²⁺ and potassium hexaniobate with heating at 343 K, gave a layered precursor film when an appropriate amount was cast onto a cover glass (18 mm × 32 mm) (see SI-2). Each ion exchange in the interlayer distance and the resulting intercalated hybrid structure were characterized by X-ray diffraction (XRD), thermogravimetric analysis/differential thermal analysis (TG/DTA), atomic force microscopy (AFM), and absorption spectroscopy. To observe the morphological changes induced in the hybrid film by photoirradiation, the central part was cut with a scalpel, and the cross-cut edge of

Received: August 3, 2011

Published: October 06, 2011

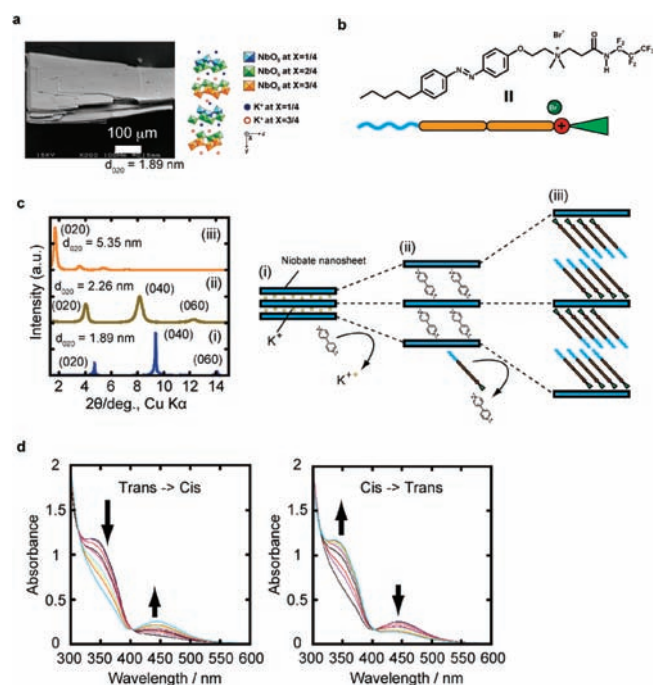


Figure 1. Chemical structure and fabrication of the hybrid film. (a) Layered structure of potassium hexaniobate. (b) Chemical structure and schematic illustration of the polyfluoroalkyl azobenzene derivative C3F-Azo. (c) XRD pattern variation. (left) The original d_{020} spacing (1.88 nm) of the starting niobate (i) expanded to 2.26 nm upon intercalation of MV^{2+} (ii), and further intercalation of C3F-Azo induced further expansion to 5.35 nm (iii). (right) Schematic illustration of niobate hybrids following guest ion intercalation. (d) Changes in the absorption spectra of the hybrid film upon irradiation with (left) UV (368 nm for 20 min) and (right) visible light (463 nm for 2 min).

the film was measured using tapping-mode AFM (SPA-300HV/SPI-4000, SII) with a silicon cantilever (SI-DF20) in ambient air. UV ($\lambda_{UV} = 368$ nm, 1.9 mW/cm²) and visible ($\lambda_{vis} = 463$ nm, 0.65 mW/cm²) light was used to irradiate the sample film through the AFM cantilever holder window for 20 and 2 min, respectively. The same area was scanned as a standard, which remained stationary. The interlayer distance change in the hybrid film was measured by XRD (RINT-TTR III, RIGAKU) before and after photoirradiation.

Figure 1c shows a schematic illustration and the corresponding XRD pattern variation of the hexaniobate compounds following the two-step guest–guest ion exchanges. The interlayer space expanded with the ion exchange, and the d_{020} spacing reached 5.35 nm in the C3F-Azo-intercalated nanosheet-stacked film. TGA/DTA provided the composition of the C3F-Azo/hexaniobate hybrid film and showed that the C3F-Azo molecules were adsorbed on the nanosheet surface at a level of ~ 2.5 times the cation exchange capacity (CEC), indicating that the area of the niobate surface occupied by one molecule of C3F-Azo was 0.31 nm². The height of the interlayer space [4.12 nm, estimated as the difference of the d_{020} spacing (5.35 nm) and the thickness of the nanosheet (1.23 nm)] and the surface area occupied by one molecule of C3F-Azo indicate that the intercalated molecules were nearly closely packed in the interlayer spaces, forming a bilayer structure with a tilt angle of 43° . Figure 1d shows the changes in the absorption spectra of the hybrid film resulting from the UV and visible-light irradiation. Reversible,

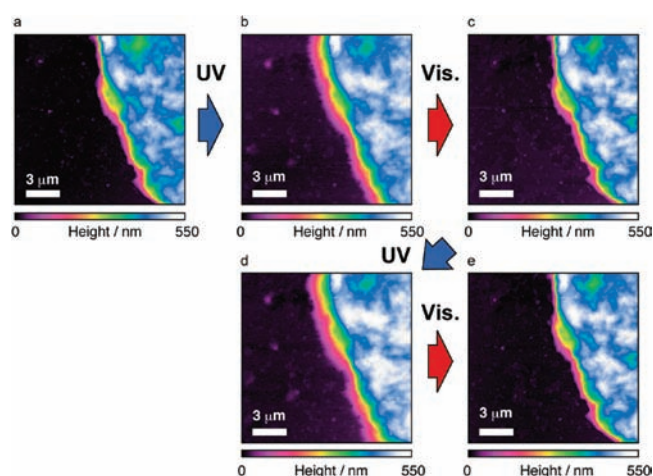


Figure 2. Morphology change in the cross-cut film edge of the layered hybrid film upon photoirradiation: topographic images of the hybrid film (a) before and (b–d) after successive irradiation with (b, d) UV (368 nm for 20 min) and (c, e) visible light (463 nm for 2 min).

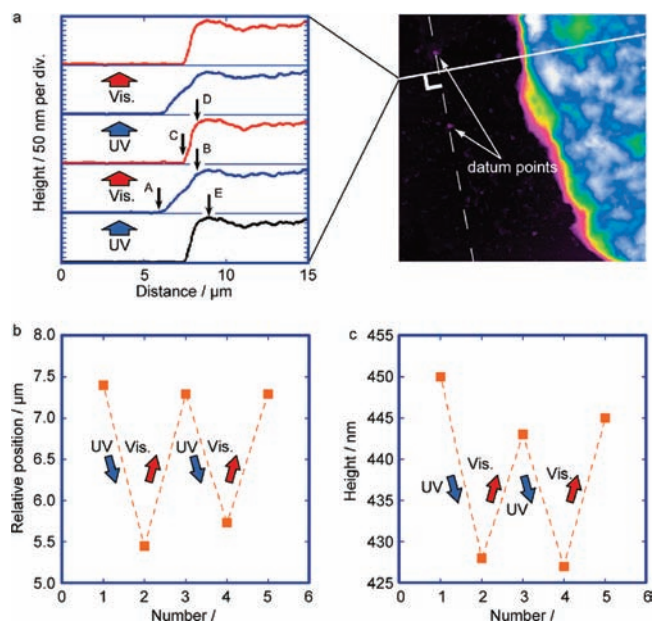


Figure 3. 3D morphology changes in the layered hybrid film. (a) Height profile of the hybrid-film cross section. (b) Relative distance from the reference point to the film edge vs number of irradiation cycles. (c) Film thickness at a point located a constant distance from the reference point vs number of irradiation cycles.

efficient photoisomerization reactions were induced by the alternating irradiations.

A reversible morphological change of the hybrid nanosheet-stacked film on a giant scale was observed upon photoisomerization. Figure 2 shows top-view AFM images of the hybrid nanosheet-stacked film fabricated by the procedure described above. To observe the film thickness and the cross section, the hybrid film was gently cut with a scalpel. The same area of the sample was scanned by AFM before and after photoirradiation. In Figure 2a, the dark part (left side) is the surface of the glass substrate, and the bright area (right side) is the top view of the layered

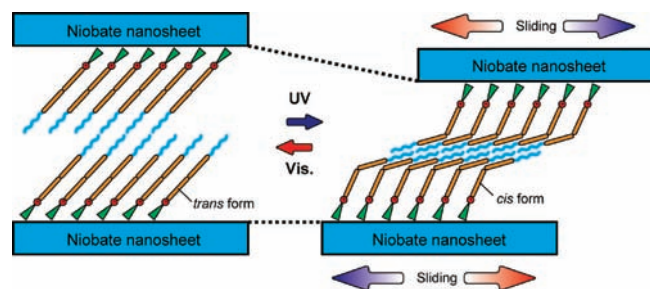


Figure 4. Schematic diagram of the niobate nanosheet sliding movement and interlayer distance change induced by photochemical trans–cis isomerization of the azobenzene molecules.

nanosheet-stacked film. UV light (365 nm) was used to irradiate the whole sample surface uniformly.

After the UV irradiation, the surface of the sample was scanned in the same area. Surprisingly, the morphology of the film, particularly the cross-cut edge region, changed dramatically in comparison with that observed before the irradiation. The edge of the bottom-most layers appeared to slide out (to the left) to a large degree (Figure 2b). Furthermore, when visible light (435 nm) was used to irradiate the sample further after it had first been irradiated with UV light, the film morphology returned to that observed before the photoirradiation (Figure 2c). These morphology changes were completely reversible (Figure 2d,e), suggesting that the niobate nanosheets were sliding in the horizontal direction relative to each other as a result of the photochemical reactions of the azobenzene derivatives intercalated in the layered structure. It is clear that the morphological change of the sliding on such a giant scale in the hybrid nanosheet-stacked film is completely different from the types of shape changes induced in single crystals and liquid-crystal polymer films.

To estimate more precisely the magnitude of the induced morphological changes, two dotlike features in the AFM image (Figure 3a, right) were taken as reference points with which to compare the relative morphological changes in the lateral direction. The height profiles along the white line perpendicular to the dashed line between the two reference points are shown in the left panel of Figure 3a. After UV irradiation, the bottom edge of the nanosheet stack (point A in Figure 3a, left) clearly slid out from the interior of the layered film structure, while the top edge (point B in Figure 3a, left) remained stationary. Furthermore, when visible light was used to irradiate the sample further, the protruded bottom edge (point C in Figure 3a, left) slid back to the original position observed before the photoirradiation. Again the top edge (point D in Figure 3a, left) did not move. The relative distance from the reference point to the most protruded film edge is plotted in Figure 3b. The back-and-forth sliding distance of the bottom edge of the film induced by photoirradiation reached ~ 1500 nm. The sliding of the photoinduced nanosheet back and forth on such a giant scale is quite interesting and unique from the viewpoint of the driving mechanism of the morphological change. The apparent linear relation between the sliding length (horizontal axis) and the height profile (vertical axis) for the blue traces in Figure 3a indicates that the sliding length is proportional to the film thickness, while the height profile of the edge before the UV irradiation (black trace in Figure 3a) rises very sharply, indicating that the cantilever well reflects the shape of the edge with enough space resolution. In

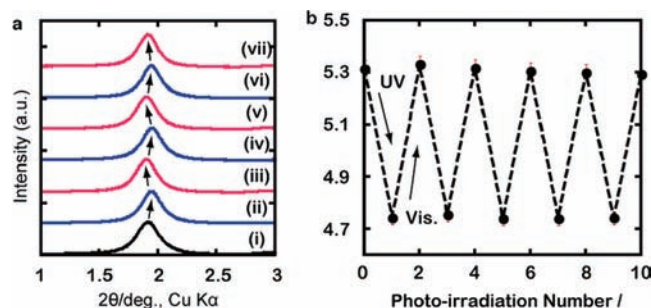


Figure 5. Reversible interlayer distance change in the layered hybrid film. (a) XRD pattern variation of the layered hybrid film by photo-irradiation (i) before and (ii–vii) after the (ii) first UV, (iii) first visible, (iv) second UV, (v) second visible, (vi) 10th UV, and (vii) 10th visible irradiation. (b) Plot of changes in the d_{020} spacing (in nm) due to photoirradiation.

the cases of organic crystals^{1,12,13} and liquid-crystal polymer films,^{3–5,14} where large morphological changes were also reported previously, the accumulation of a number of small conformational changes due to photochemical reaction in the highly ordered system gives rise to the large shape change at the macroscopic level.

On the other hand, in the case of the organic/inorganic nanosheet-layered film reported here, it is considered that the nanosheet sliding motion can be induced by efficiently sweeping away from the opposite side C3F-Azo molecular alignment in the bilayer structure in the horizontal direction when photochemical trans–cis isomerization of the molecules is induced, as shown in Figure 4. Each nanosheet stacked on the glass plate was situated parallel to the glass surface. The number of layers was estimated to be ~ 84 ($450 \text{ nm}/5.35 \text{ nm}$), so the lateral motion per layer was estimated to be $1500 \text{ nm}/84 \text{ layers} = 17.9 \text{ nm/layer}$. The cooperative, anisotropic motion of C3F-Azo, which formed a closely packed bilayer structure with an ordered molecular alignment on the niobate nanosheet, presumably induced the morphological change of the layered film. The most curious point is that this reversible morphological change of the stacked nanosheet film is a phenomenon very similar to that for muscle contraction and relaxation, which is induced by a sliding actin filament with the consumption of chemical energy [i.e., adenosine triphosphate (ATP)] in the human body.^{16,17} The hybrid film, on the other hand, utilizes photon energy to realize the sliding morphological change.

Very interestingly, the hybrid film also underwent changes in the morphology in the vertical direction, in addition to the lateral nanosheet sliding. The film thickness at the position far from the reference point with a constant distance in the AFM images (point E in Figure 3a, left) is plotted in Figure 3c. The hybrid film shrank and expanded also in the vertical direction up to ± 18 nm upon UV and visible-light irradiation, respectively. The maximum height increase was $\sim 4\%$. Thus, the 3D morphological changes of the nanosheet sliding and the film thickness change were attained simultaneously through the photoisomerization of azobenzene.

Another most curious point should be the question of how the horizontal sliding and the vertical expanding/shrinking are induced and how the morphological changes on such a giant scale are correlated with the trans–cis isomerization of each C3F-Azo molecule. To gain a deeper insight into this point, the interlayer distance change of the layered hybrid film was inspected. The XRD

pattern variations of the layered hybrid film upon photoirradiation are shown in Figure 5a. The diffraction peak was shifted to higher angle by UV irradiation, i.e., the interlayer distance of the layered hybrid film decreased as a result of isomerization from the trans to the cis form of azobenzene upon UV irradiation. On the other hand, the diffraction peak shifted back to the original position after the subsequent visible-light irradiation. Thus, the interlayer spacing of the hybrid film shrank and expanded because of the repeated UV and visible-light irradiation (Figure 5).

It is clear that the macroscopic morphological change of the nanolayered stacked film in the AFM analyses is accumulated with the change of each interlayer distance. It should be noted here that the interlayer distance decreased by >10% while the macroscopic film thickness decreased by only 4%, presumably as a result of an incomplete change in the bottom layers due to incomplete isomerization. It is considered that the cooperative photoisomerization reactions in the interlayer spaces induce each nanosheet sliding and interlayer distance change, which give rise to the 3D morphological change. The variation of the d_{020} spacing of the hybrid film upon irradiation with UV and visible light in turn is shown in Figure 5b. The shrinkage and expansion of the interlayer spaces was induced repeatedly. Why such a giant sliding in the vertical direction in a reversible manner is induced and how the vertical and horizontal motions are correlated with each other are most intriguing questions. Though the detailed mechanism is not yet fully understood, the way that the azobenzene molecules align in the microenvironment should be one of the key factors in the presumed cooperative effects among the adjacent molecules within the same layer along with the opposite ones in another layer in the bilayer structure. The polyfluorinated propyl group should also contribute the most crucial role, since the corresponding hydrocarbon analogue of the azobenzene surfactants do not show such 3D motions. A detailed mechanistic study focusing on those points is now in progress and shall be reported elsewhere.

It is suggested that the reversible nanosheet sliding and thickness change of the present hybrid film could eventually be a novel model for the conversion of photon energy to mechanical energy. This phenomenon may also provide a great impact to the design and construction of light-driven actuators as artificial muscles, based on a new driving mechanism.

■ ASSOCIATED CONTENT

S Supporting Information. Synthesis of C3F-Azo and an AFM image of the MV^{2+} - $K_4Nb_6O_{17}$ hybrid. This material is available free of charge via the Internet at <http://pubs.acs.org>.

■ AUTHOR INFORMATION

Corresponding Author
inoue-haruo@tmu.ac.jp

■ ACKNOWLEDGMENT

This work was partially supported by a Grant-in-Aid for Scientific Research on Priority Area "New Frontiers in Photochromism (No. 471)" from the Ministry of Education, Culture, Sports, Science and Technology of Japan.

■ REFERENCES

- (1) Kobatake, S.; Takami, S.; Muto, H.; Ishikawa, T.; Irie, M. *Nature* **2007**, *446*, 778.
- (2) Irie, M.; Kobatake, S.; Horichi, M. *Science* **2001**, *291*, 1769.
- (3) Yu, Y.; Nakano, M.; Ikeda, T. *Nature* **2003**, *425*, 145.
- (4) Yamada, M.; Kondo, M.; Mamiya, J.; Yu, Y.; Kinoshita, M.; Barrett, C. J.; Ikeda, T. *Angew. Chem., Int. Ed.* **2008**, *47*, 4986.
- (5) Yamada, M.; Kondo, M.; Miyasato, R.; Naka, Y.; Mamiya, J.; Kinoshita, M.; Shishido, A.; Yu, Y.; Barrett, C. J.; Ikeda, T. *J. Mater. Chem.* **2009**, *19*, 60.
- (6) Irie, M.; Fukaminato, T.; Sasaki, T.; Tamai, N.; Kawai, T. *Nature* **2002**, *420*, 759.
- (7) Irie, M. *Chem. Rev.* **2000**, *100*, 1685.
- (8) Bian, S.; Liu, W.; Williams, J.; Samuelson, L.; Kumar, J.; Tripathy, S. *Chem. Mater.* **2000**, *12*, 1585.
- (9) Natansohn, A.; Rochon, P. *Chem. Rev.* **2002**, *102*, 4139.
- (10) Nakano, H. *J. Phys. Chem. C* **2008**, *112*, 16042.
- (11) Isayama, J.; Nagano, S.; Seki, T. *Macromolecules* **2010**, *43*, 4105.
- (12) Koshima, H.; Ojima, N.; Uchimoto, H. *J. Am. Chem. Soc.* **2009**, *131*, 6890.
- (13) Morimoto, M.; Irie, M. *J. Am. Chem. Soc.* **2010**, *132*, 14172.
- (14) Wang, D. H.; Lee, K. M.; Yu, Z.; Koerner, H.; Vaia, R. A.; White, T. J.; Tan, L.-S. *Macromolecules* **2011**, *44*, 3840.
- (15) Nassau, K.; Shiever, J. W.; Bernstein, J. L. *J. Electrochem. Soc.* **1969**, *116*, 348.
- (16) Eisenberg, E.; Hill, T. L. *Science* **1985**, *227*, 999.
- (17) Yanagida, T.; Arata, T.; Oosawa, F. *Nature* **1985**, *316*, 366.